

Boat-Generated Wave Measurements in The Connecticut River

Y. Ozeren & M. Altinakar

National Center for Computational Hydrosciences and Engineering, University of Mississippi, University, MS, USA

A. Simon

Natural Resources & Health Sciences Division, Cardno, Oxford, MS, USA

ABSTRACT: Boat-generated waves can have significant contribution to bank erosion along inland streams and waterways. Waves generated by the frequent passes of high-speed boats in shallow waterways can substantially increase local velocities, sediment concentration, and turbidity. Wave induced erosion can reduce the stability of riverbanks and induce bank failure. In order to accurately predict wave induced bank erosion, and associated damage to the streambanks, boat traffic and the characteristic of the generated waves must be known. In this study, boat-generated wave properties were measured at three sites along a section of the Connecticut River. Each measurement station consisted of one or more wave loggers to measure the water surface displacement, and two time lapse cameras to capture the boats as they pass. In this paper, the wave logger data analysis procedures, boat statistics and wave properties during the measurement period are presented. The results show that, the waves generated by high-speed recreational boats are much larger than the wind generated waves and their potential impact on the riverbanks can be substantially higher than that of the river flow.

1 INTRODUCTION

Boat-generated waves can significantly contribute to shoreline erosion, increase suspended sediment concentration, and turbidity, and induce streambank failure. Measurements in Kenai River in Alaska showed that the energy transmitted to the banks from boat waves is up to 60% of energy of the streamflow (Maynard, 2008). Due to the increasing popularity of recreational vessels in recent years, boat induced wave erosion has become a major concern in rivers (Figure 1). In order to predict the bank erosion and associated damage to the streambanks, the characteristic of the boat-generated waves must be known.

This study concerns field measurement of boat traffic and boat-generated wave properties in the Connecticut River. Three field-monitoring sites were installed along a reach of Connecticut River between Vernon Dam, Vernon, VT and French King Bridge, Miller Falls, MA. Each measurement station consisted of a wave logger to measure the water surface displacement, and two time-lapse cameras to capture the boats as they pass. This paper presents wave-logger data analysis procedures and measured wave properties, along with the boat traffic statistics during the 116-day long field campaign.

2 THEORETICAL BACKGROUND

A boat traveling across the water surface generates waves that propagate away from the bow. The wave system during the interaction between the boat and water can be divided into two components: primary and secondary waves. Primary wave (drawdown) is the single standing wave relative to the ship between the bow and the stern. The impact of primary waves on the banks depends on the ratio of the boat cross-sectional area perpendicular to the sailing line, to the river flow cross-sectional area. Primary waves can be neglected for small values of this ratio (Goransson et al., 2013).

Secondary waves are caused by the disturbances due to the acceleration of the water around the ship



Figure 1. A high-speed boat operating near SR-10 Bridge, MA.

(Bertram, 2000). Secondary wave pattern consists of symmetrical pairs of divergent waves traveling obliquely out from the sailing line, and transverse waves traveling in the direction of the sailing line.

Figure 2 shows the geometry of the secondary waves system in deep water. Divergent waves move out from the sailing line on both sides with an angle θ , and transverse waves move along the sailing line. The interaction of divergent and transverse waves form a line of maximum wave heights, called cups, which extends on each side of the sailing line at an angle of β . The period of these waves stay constant while their height decrease as they travel away from the bow. Since transverse waves travel parallel to the sailing line, and attenuate at a faster rate compared to the divergent waves, their impact on the stream banks is relatively low.

Divergent wave system can simply be defined by the wave period, T , (or wavelength, L), wave height, H , and direction of wave propagation. Wave period and direction of propagation depend only on the relative vessel speed and water depth, whereas wave height is a function of several parameters including the velocity of the flow relative to the vessel, shape of the boat, distance of the boat from the shoreline, channel width and water depth. Even though wave period and direction of wave propagation can be estimated using analytical methods, empirical relations are often needed for wave height estimation (Sorensen, 1997; Kriebel and Seelig, 2005). A depth based Froude number is defined as:

$$F_h = V_B / \sqrt{gh} \quad (1)$$

where V_B is the boat speed, g is gravity and h is the local water depth. Froude number, F_h characterizes the secondary wave pattern depending on whether it is deep or shallow water waves.

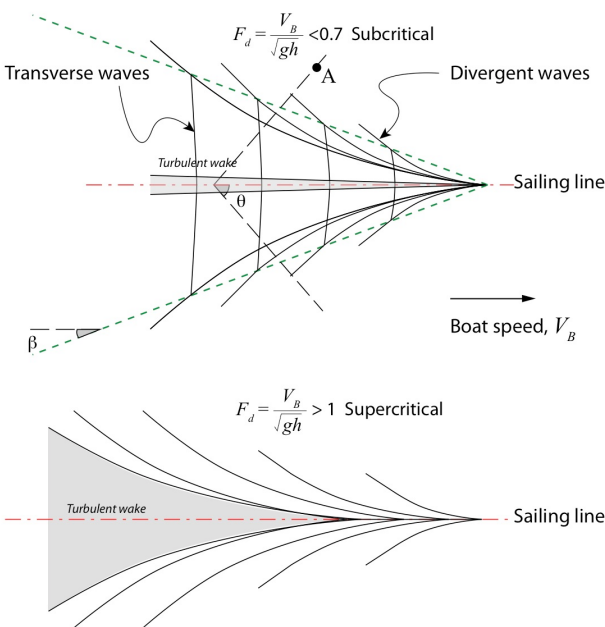


Figure 2. Definition sketch of the boat generated waves at subcritical and supercritical speeds.

In Figure 2, the wave record measured at point "A" located in deep-water consists of a leading small height and long period waves followed by larger waves of shorter periods, which gradually decays to smaller waves. The wave signature of a boat passage is most commonly characterized by the maximum wave height.

3 FIELD SITES AND INSTRUMENTATION

Three boat monitoring sites were installed along the 32 km-long river reach in the Connecticut River between Vernon Dam (Hinsdale, NH) and Turner Falls Dam (Montague, MA). The monitoring sites were selected based on the availability of camera installation sites suitable for boat monitoring. Figure 3 shows a map of the study area and a graph that shows the relative distances between the sites. Six cameras were installed on three bridges along the river reach to have ease of access and sufficiently wide field of view.

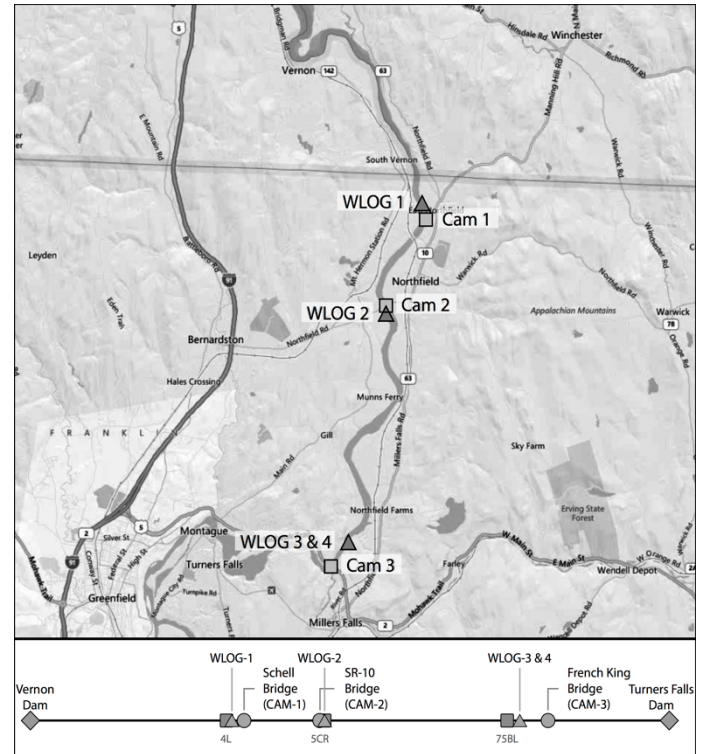


Figure 3. Boat monitoring site locations.

The wave loggers were held in place by a T-post driven into the riverbed near the bank at each site. Two upstream sites were equipped with one wave logger (WLOG-1 and WLOG-2) while the downstream site had two wave loggers (WLOG-3 and WLOG-4) for wave direction estimation. The logger stations were chosen close to the riverbanks with the objective to measure the boat-generated waves near the shore before they shoal and break. Each wave logger consisted of a capacitance type wave staff and a battery powered microprocessor that stores the water level. The 2-m-long staffs had a vertical resolution of

approximately 0.5 mm. The loggers were operated continuously at a sampling frequency of 30Hz, which provided a fairly good temporal resolution for the type of boat waves measured in this study (approximately 15-readings-per-wave). Staffs were secured to the T-posts at 2/3 of their heights to limit their motion. The elevation of the mid-height of the staffs was aligned with the 15-year average median stage of the river at each installation site. The recoded data was downloaded at two-week intervals in order to avoid unexpected data loss.

Each field site was equipped with two different types of consumer-grade camera. A wide-angle camera (115° Field of view) served as the primary camera while the other one with a narrower field of view (50°) was used as the secondary camera for close-up pictures when needed. Both cameras were configured to take pictures at 10-second intervals at a pixel resolution of 1280 by 720 between 6 am and 9 pm. Data from the cameras were downloaded at every two weeks.



Figure 4. Wave loggers WLOG-3 and WLOG-4.

4 DATA ANALYSIS

Boat waves were recorded continuously at four loggers between May 22nd, 2015 and September 14th, 2015. Quantitative boat traffic statistical data and boat generated wave data were obtained mainly from the wave logger data analysis. Camera recordings were used to visually supplement the wave analysis and to validate the boat signatures detected in the wave data. Rain events were also acquired from the video recordings.

Wave logger data is stored in an ASCII file containing the water surface elevation at 30Hz data rate. Raw data was converted to actual elevations using the linear calibration curves, and transformed to a reference vertical datum (NAVD88, US feet) through RTK GPS survey of the loggers. The time series at four-wave loggers were analyzed to obtain mean water level and water-surface displacements during the monitoring period. Daily signal was filtered using a

low-pass IRR (internal impulse response) filter of order 10 and with a 10 s cut-off length to remove high frequency components including the boat and wind waves. The original signal was normalized with the filtered signal to obtain water surface fluctuations. The high frequency ripples and noise were removed using another low-pass filter, of order 10 and cut-off length.

Figure 5 shows a sequence of pictures recorded at CAM-2, and the time series of the water surface displacement of the boat recorded at WLOG-2 (see Figure 3). The camera looking in the downstream direction was taking one picture every 10 s. The arrows in the pictures in Figure 5 specify the WLOG-2 location. As seen in these pictures, the wave pattern behind the boat is relatively narrow and without any transverse waves which indicates that the boat was travelling at supercritical speed ($F_h > 1$). Also in Figure 5, the lag between the time that the boat appears in the camera field-of-view in three pictures, and the time of the maximum wave height in the time series plot is related to the propagation speed of the wave group.

The time series data at fixed gauge locations showed that, boat wave signals appear as short, low to high frequency chirps superposed onto the random wind waves. This distinct characteristics was used to identify them in the recorded signal. Waves with different frequencies travel with different speeds in water. At a stationary point, the recoded wave signal shows a wave group gradually shifting from low to high frequency, due to frequency dispersion. This transient wave group has a unique oscillatory pattern, and usually much more energetic than irregular wind-generated waves. The wave amplitude increases as the wave frequencies increase until peak wave amplitude is reached.

The time history of the frequencies of a transient boat wave signal was found using local time-frequency analysis. Both wavelet transform and windowed Fourier transform were tested for their performance during the preliminary tests. Wavelet transform uses inner products to measure the similarity between the time series signal and a wavelet function. The resulting transformation is visually represented by a scalogram. Windowed Fourier transform divides the signal into segments, and each segment is transformed into Fourier space using a window-function. The time series signal is decomposed into its time-frequency-spectral density components, which is visually represented by a spectrogram. The spectrogram is a function of both the frequency and time since the decomposition is local. In the current study, both methods produced similar results in detecting boat generated waves in the recorded signal. Windowed Fourier transform, however, was relatively faster than the wavelet transform; therefore, it was adopted here.

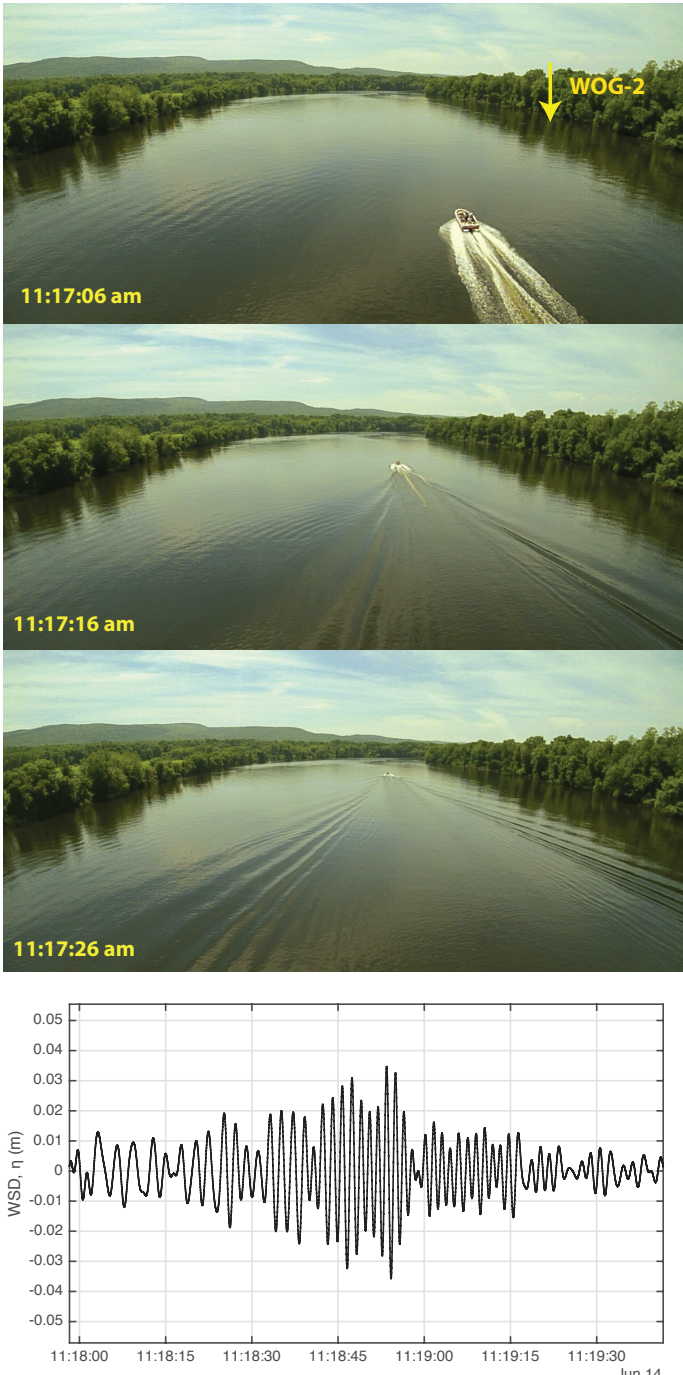


Figure 5. An example boat record and the corresponding wave time series.

Figure 6 illustrates a typical wave measurement signal and its spectrogram. The spectrogram is obtained using a Hamming windowed Fourier transform, of 512 (number of data points in the 30Hz signal) with 75% overlapping. The low frequency to high-frequency chirp pattern can be easily identified.

Using the spectrogram, individual boat passes were identified in the frequency domain. The locations of the maximum wave heights and the wave frequencies associated those waves were obtained in each boat wave signal using zero-crossing analysis. Each wave is defined between two successive zero down-crossings in the normalized signal. The wave height is the difference between the maximum and minimum water surface displacement and the wave period is the time length of each wave.

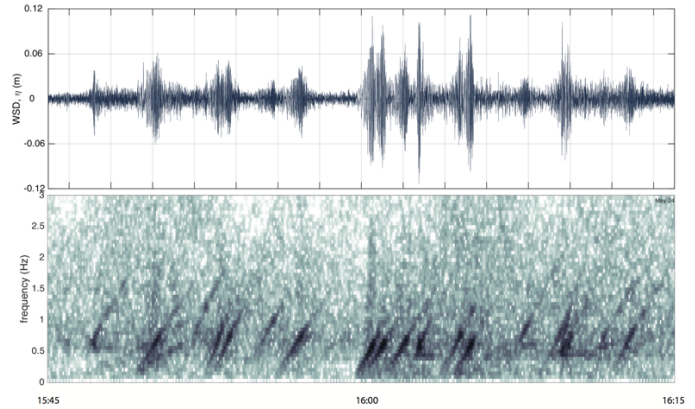


Figure 6. Recorded wave signal and its spectrogram on May 24, 2015, 3:45pm – 4:15pm at wave logger 4.

Unlike the regular boat generated waves, wind generated waves are irregular; therefore, they are described by spectral quantities rather than individual wave properties. Wind waves are narrow banded for limited fetch conditions and their distribution of wave heights closely follows the Rayleigh distribution. Significant wave height can be approximated by the standard deviation (square root of the variance of the signal) (Longuet-Higgins 1952).

$$H_{mo} = 4.004\sqrt{m_o}, \quad (2)$$

where m_o is the zero-th moment of the spectrum. These differences between the characteristics of boat generated waves and wind waves are used to filter the boat waves and identify boat passes in the recorded signal.

Summary of the wave data analysis

The major steps of the wave data analysis and boat detection procedures are listed below:

- Separate the water surface fluctuations, $\eta(t)$, and mean water level, $z(t)$, from in the measured water level signal using a low pass IRR filter.
- Apply windowed Fourier transform to find the spectrogram $S(t, f)$ (Hamming window of size 512 with 75% overlap. The windows are 17s long and 4.3s apart, center-to-center)
- Find the mean spectral density, $\bar{S}(t)$, in the low frequency band 0.05Hz-0.8Hz. Most of the wind-generated waves are left on the high-frequency side of this range.
- Remove low-frequency modulations in $\bar{S}(t)$ using a third-order Savitzky-Golay filter.
- Find the peaks and their locations (t_{peak}) in the filtered $\bar{S}(t)$ time-series. The locations are defined as the window centers.
- Filter the high frequency components in the water surface fluctuations $\eta(t)$ with a low pass IRR filter and isolate waves in the frequency range of 0.1Hz - 2.5 Hz.
- Using zero-crossing analysis, calculate the wave height $H(t)$ and wave period $T(t)$ timer series.

- Calculate the spectral estimate for the significant wave height H_{m0} using the Equation 1.
- Find the peak zero-crossing wave heights H_{max} and wave periods T_{max} , nearest to t_{peak} .
- Compare the results with the time-lapse videos and remove any false detection.

The data recorded at three sites (four loggers) was analyzed following the procedure described above. The procedure is automated except the final step in which the detected boat waves are compared with the time-lapse videos. Overlapping waves due to simultaneous boat passes, very small waves falling below the thresholds, and high wind waves that were detected as boat waves were the most common causes of boat detection errors. These errors were identified and removed using the time-lapse videos and the spectral analysis. The water level rarely exceeded the maximum or minimum measurable height of the loggers. Those instances were excluded from the statistical analysis.

5 RESULTS AND DISCUSSIONS

The procedure described in the previous section was used to calculate the boat traffic statistics and the wave properties at each logger. Figure 7 summarizes the results of one daylong analysis. The data was collected on June 14th, 2015, Sunday at WLOG-3. The Figure consists of three plots: the one on top is the mean water depth and water surface elevation (NAVD88, US Feet) on the secondary axis, the middle plot is the water surface displacement, significant wave height, the zero-crossing wave amplitude, and the temperature (secondary axis), and the bottom one is the spectrogram, which shows the spectral energy, frequency and time relationship. The temperature sensors were in the wave logger enclosure; therefore, they overestimated the temperature during daylight. The temperature data was qualitatively used to identify the sunny and cloudy or rainy days in the dataset. 190 boats passes were detected for the day shown in Figure 7. The boats appear as short bursts in spectrogram and the their energy is widely distributed over a wide range of frequency, peaking around 1 Hz. Detected peaks are marked with ‘plus’ signs in both wave time series and spectrogram plots. The positions of these plus signs on the vertical axis show the peak frequency of the waves. Most of energy is concentrated around this frequency. The wind generate wave were less pronounced compared to the rest of the data recorded at the same site. The water depth increased from 2.6 m to 3.6 m throughout the day.

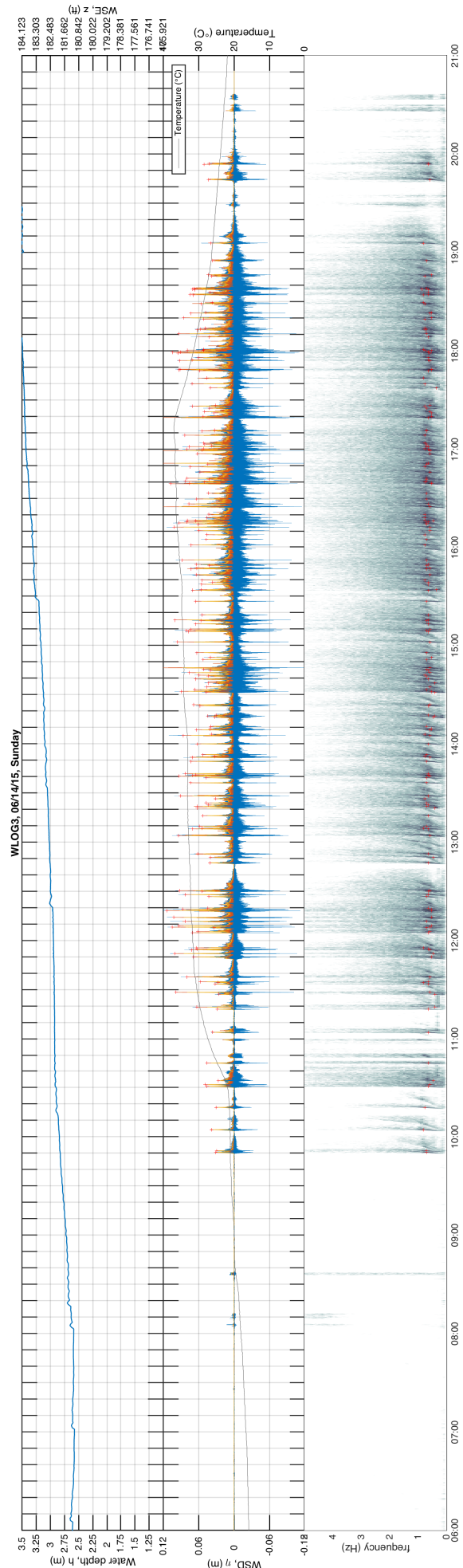


Figure 7. Wave data analysis summary for WLOG-3.

The total number of boats estimated from the wave logger data analysis is listed in Table 1. 12,148 boating events were recorded at three sites during the 117-days data collection period. WLOG-3 and WLOG-4 (French King Bridge site) had the busiest boat traffic compared to the other two locations.

Table 1. Total measured number of boats

Wave logger	Dates	Number of boats
WLOG-1	May 21 – Aug 28	2133
WLOG-2	May 21 – Sep 14	2650
WLOG-3	May 21 – Sep 14	7365
WLOG-4	May 21 – Sep 14	7263

Figure 8 illustrates the daily distribution of the boat traffic during the data collection period between May 22nd, 2015 and September 14th. Sundays and holidays are designated with dark tones. Daily maximum and daily minimum temperatures are also plotted in the same figures. The analysis results show that the boat traffic can exceed 200 boats for some days. Weekends, especially Sundays, have significantly higher daily traffic than the weekdays. During rainy days boat traffic dropped significantly regardless of the day of the week. Highest number of boat passes was 239, which was observed on July 5th, the Sunday after the Independence Day. Note that the number of boat passes on 4th of July is much less due to the rainy weather conditions.

In summary Figure 8 show that, daily traffic depends primarily on the day of the week, precipitation or weather conditions, and location along the river. There is no noticeable trend between different months; nonetheless, the traffic is relatively low in June, which may be due to relatively frequent rain events.

Mean daily boat traffic flow at WLOG-3 site per each day of the week is plotted in Figure 9. The bar chart in this figure also compares the total daily traffic flow with rainy day traffic flow. The highest traffic flow is observed on Sunday. The lowest mean boat traffic flow is during the weekdays, Monday to Thursday (MTWT). The traffic flow rate begins increasing on Friday and peaks on Saturday on dry days. WLOG-3 site with the statistics shown in this figure has the highest mean daily traffic reaching up to 180 boats per day on dry Sundays. The highest mean traffic flow at WLOG-1 site was less than 60 boats on dry Sundays.

Boat traffic flow strongly depends on the rainfall events regardless of the measurement site. Figure 10 compares the total number boats observed on rainy and dry days, and on Sundays and weekdays for WLOG-3. Error bars are the standard deviations of the data. The mean traffic flow drops as low as 10% if it rains on Sundays and %20 on a weekday. The uncertainty of the average traffic flow is higher on weekdays because of the limited number of boating

events. Similar results are obtained at the other wave logger sites.

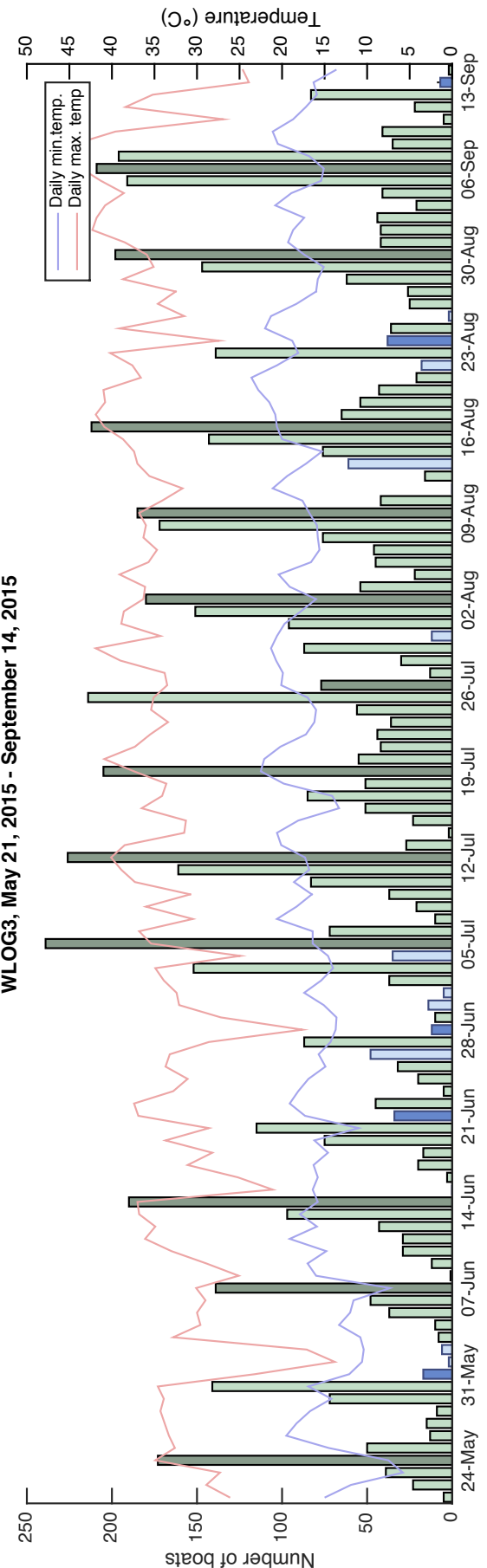


Figure 8. Boat traffic statistics at WLOG-3 between May 21st and Sep 14th

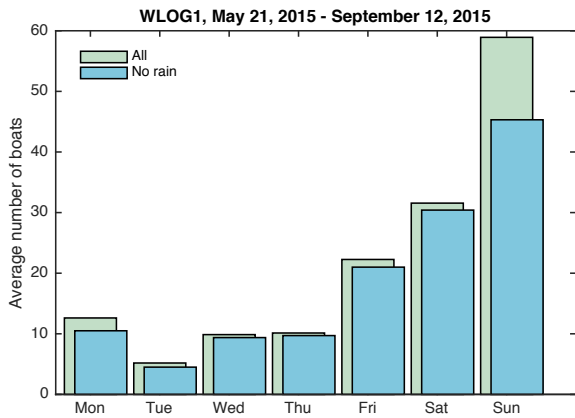


Figure 9. Day of the week boat traffic mean flow: Dry and rainy days

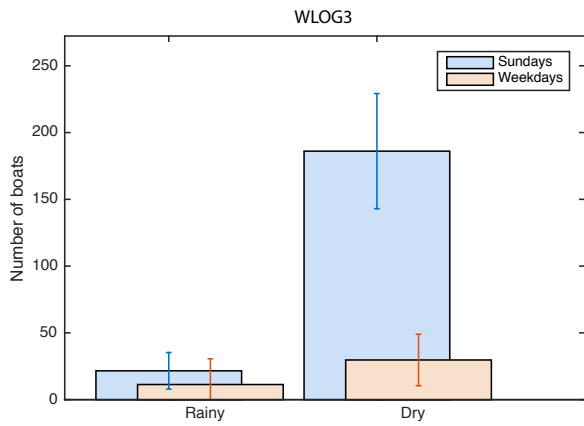


Figure 10. Average rainy and dry day boat traffic flow: Sundays and weekdays.

Figure 11 shows the hour-of-the-day distribution of the average boat traffic at WLOG-3 site. The chart is based on the whole dataset including the rainy days. Highest number of boat passes was observed between 12 pm and 8 pm peaking around 1 pm. Hourly peak traffic flow rate ranged between 2.5 and 8. The double peak can be related to the direction of the traffic flow during different time of the day. No double peaks were observed at the other sites.

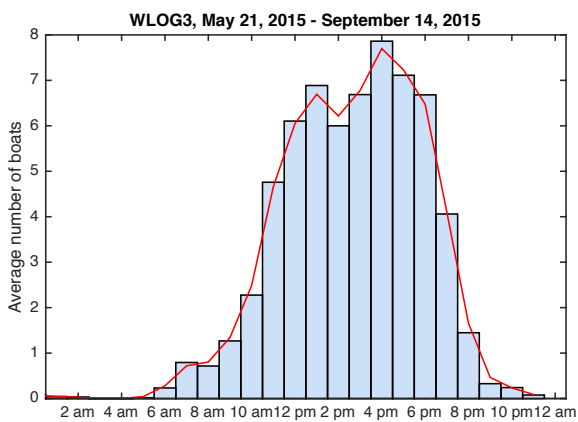


Figure 11. Hourly distribution of the boat traffic flow.

Although the wave logger data did not provide information about the wave propagation or boat direction, the time-lapse videos suggest that the boats were mostly traveling upstream in the morning hours, and downstream in the afternoon hours. The fact that downstream of the study site WLOG-3 is more populated and has higher number of boat ramp accesses compared to the upstream supports this conclusion. The upstream traffic peaks around 2 pm while downstream traffic peaks around 5 pm.

The distribution of the wave parameters wave height, H_{max} and wave period, T_{max} , and the water depth, h at WLOG-3 site is shown in Figures 12, 13, and 14. Some known probability distribution models are fitted to these histograms (water depth: normal distribution, wave period: burr distribution, and wave height: inverse Gaussian distribution). The mean water depth was 2.8 m as shown in Figure 12. The staff length limits the higher end of bar chart. Lowest water level is around 1.5 m. The average wave period of the highest wave was approximately 1.4 s (Figure 12). Wave periods of most of the detected boats are less than 2 s and greater than 1 s.

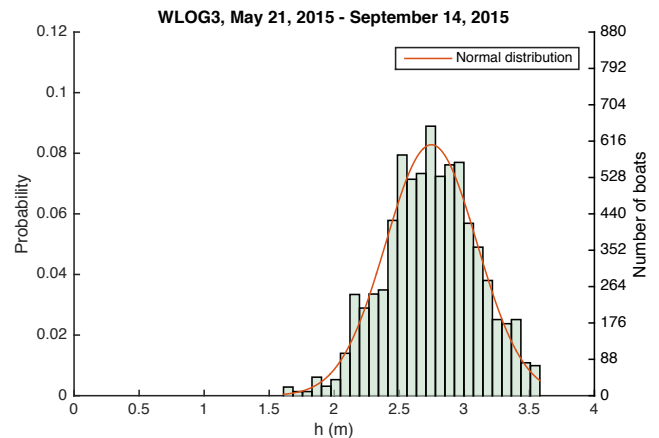


Figure 12. Water depth distribution

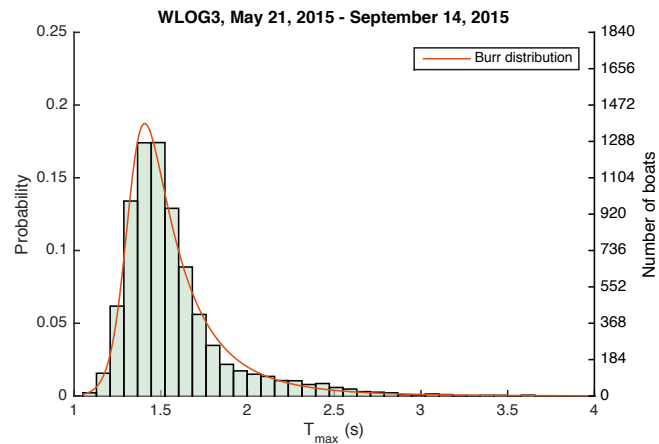


Figure 13. Maximum wave period distribution

The average maximum wave height recorded at WLOG-3 is around 7 cm - 8 cm (Figure 14). Wave of height 25 cm or more was rarely observed during the

study period. Both wave height and wave period histograms are skewed to the left.

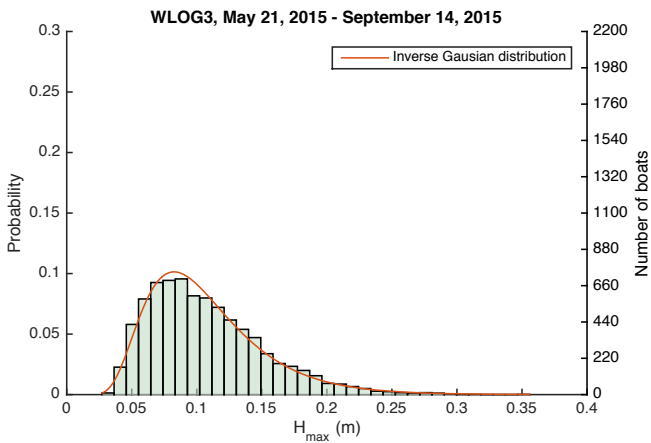


Figure 14. Wave height distribution.

REFERENCES

- Gharbi, S., Valkov, G., Hamdi, S., and Nistor, I. "Numerical and field study of ship-induced waves along the St. Lawrence Waterway, Canada." *Nat. Hazards*, 54(3), 605–621, 2010
- Kriebel, D. L., and Seelig, W. N. 2005 "An empirical model for ship-generated waves." Proc., 5th Int. Symp. on Ocean Wave Measurement and Analysis, Madrid, Spain
- Sorensen, R. M. 1997, "Prediction of vessel-generated waves with reference to vessels common to the Upper Mississippi River System." ENV Rep. 4, U.S. Army Eng. Waterways Experiment Station, Vicksburg, MS
- Maynard, S. T., Biedenharn, D. S., Fischenich, C. J., & Zufelt, J. E. 2008 "Boat-wave-induced bank erosion on the Kenai River, Alaska", (Göransson et al., 2013)
- Bertram, V. 2000. *Practical ship hydrodynamics*, Butterworth-Heinemann, Oxford, U.K.
- Göransson, G., Larson, M., & Althage, J. 2013. Ship-generated waves and induced turbidity in the Göta Älv River in Sweden. *Journal of Waterway, Port, Coastal, and Ocean Engineering*, 140(3), 04014004.
- Longuet-Higgins, M. S. 1952. On the statistical distributions of sea waves. *J. mar. Res.*, 11(3), 245-265.

6 CONCLUSIONS AND FUTURE WORK

Three boat and wave-monitoring stations were installed at three locations along the reach of Connecticut River between Vernon Dam and turner Falls Dam. The stations consisted of wave loggers and time-lapse cameras. Continuous wave data was collected for over four months between May and September of 2015. A chirp detection method was used to identify boats and wave properties. The data was used to obtain boat traffic and wave statistics at the tree sites.

Time-lapse video analysis revealed that the majority of the boat traffic consists of 6 m to 9 m-long high-speed recreational vessels moving at supercritical speeds. Highest boat traffic was observed between noon and 8 pm. Average maximum wave height was 7 cm - 8 cm m and the corresponding wave periods averaged around 1.4 s. The daily traffic flow peaked on Sundays, whereas rain significantly reduced the number of boats observed on a given day.

The available time-lapse videos can be used to estimate some of the key parameters including type and size of the boat, speed, distance to the shoreline. These parameters can be combined with the wave data to develop an empirical boat wave prediction model. The results can also provide data for the calibration of the existing boat-wave prediction models. Therefore, future work will include development of image processing techniques for boat detection and development of an empirical boat wave prediction model.